Reassessment of paleointensity estimated of a single lava flow from Xitle volcano, Mexico, by means of multispecimen domain-state corrected

L.M. Alva-Valdivia, M.A. Bravo-Ayala, P. Camps, A.N. Mahgoub, Thierry Poidras

Multispecimen domain-state corrected paleointensity determination of a detailed single lava flow, Xitle volcano (Mexico)

L. M. Alva-Valdivia[1*], M. A. Bravo-Ayala[1], P. Camps[2], A. N. Mahgoub[1,3], and Thierry Poidras[2]

[1] Laboratorio de Paleomagnetismo, Instituto de Geofísica, Universidad Nacional Autónoma de México, C.P. 04510, Coyoacán, México

[2] Géosciences Montpellier, CNRS and University Montpellier, Montpellier, France

[3] Geology Department, Assiut University, Assiut 71516, Egypt

*Corresponding author: lalva@igeofisica.unam.mx

Abstract

Determining paleomagnetic field intensity (paleointensity: PI) for lavas with high reliability and low measurement uncertainty is still difficult to achieve. In addition to the factors on which the PI used methods depend, this could be attributed to some non-ideal physical and magnetic characteristics of lava sample, including grain size, cooling rate effect, and thermal stability. Xitle volcano (SW Mexico City) is a good example to illustrate and discuss this problem because dozens of previous PI studies were carried out on its evolved flow units, which have commonly resulted in different mean values with large dispersions. Indeed, *211* published PI data obtained by use of Thellier and microwave experiments gave a mean of *64.1 μT* with a standard deviation of *11.0 μT*. After a careful evaluation, we found that only *134* of these data can be considered reliable, as they meet a set of selection criteria designed

in this study. These evaluated data gave an average mean of $62.0 \pm 9.3\ \mu T$. In order to strengthen the PI estimates of Xitle, we conducted a multispecimen domain-state corrected (MSP-DSC) method along one vertical (~ 4.5m) and three horizontal (~ 1.25m, each) profiles. Top horizontal and vertical profiles have fulfilled a stringent criteria set while central and bottom profiles exceeded the alteration check criteria limit and thus are considered unreliable. Accordingly, Xitle PI mean derived from MSP-DSC experiment is calculated at $60.5 \pm 4\ \mu T$, thus in a good agreement with the mean value estimated from previous filtered data. The result and success rate obtained may be ascribed to cooling rate variations commonly found at the lava profile, and indicate that MSP-DSC outcome is governed by the magnetic properties such as the domain-size behavior and the thermal stability of the magnetic carriers present in the treated specimens, as in the conventional Thellier & microwave-style experiments. From these two averages, a combined mean and standard deviation of $61.9 \pm 9\ \mu T$ is calculated, which technically is considered the most probable intensity estimate at the Xitle eruption time, $ca.$ 370 AD.

Keywords: paleointensity; lavas; rock magnetic properties; multispecimen method; Xitle; Mexico

1. Introduction

Over the long history of our planet, the magnetic field generated in the liquid outer core changed on different time scales from years to billions of years. Understanding the spatio-temporal evolution of this field requires careful determination of its strength. Because of its large contributions in deciphering the geodynamo behavior (Biggin et al., 2012) and improving the global geomagnetic field models (e.g., SHA.DIF.14k, Pavón-Carrasco et al., 2014), several methods were proposed to obtain a reliable estimate of the PI: the classical

Thellier-Thellier experiment (Thellier & Thellier 1959) and other protocols (e.g., Coe et al., 1967; Aitken et al., 1988; Tauxe and Staudigel, 2004); the Shaw method (Shaw, 1974) and its variants (e.g. Tsuanakawa and Shaw, 1994); pseudo-Thellier (Tauxe et al., 1995); the microwave technique (Hill & Shaw 1999); and the recent approach of multispecimen (Biggins and Poidras, 2006; Dekkers and Böhnel, 2006; Fabian and Leonhardt, 2010). Despite the improvements achieved in the laboratory protocols, these methods give reliable intensity with a low success rate (generally less than 30%) from basalts, the material of interest in this study. This was showed by comparing PI data retrieved from historically erupted lava flows, such as those in Hawaii (e.g. Yamamoto et al., 2003; Böhnel et al., 2011; Grappone et al., 2019) and Etna (e.g. Hill and Shaw, 1999; De Groot et al., 2013), with the actual geomagnetic field intensity that is well known from geomagnetic observatories. Th elow success rate in the PI methods to recover the expected field intensity with high accuracy could be attributed to several reasons, including the presence of non-ideal physical and magnetic properties, magneto-mineralogical alteration, the cooling rate difference and presence of local magnetic field effects (Stacey & Banerjee 1974). From the PI point of view, lava samples must contain ferromagnetic particles of single domain (SD; < ~80 nm) to pseudo-SD (PSD; < ~0.1 μm) size . This condition however, is not easily reached because in naturally cooled lavas there are always contributions from grains larger than ~1.0 μm, of multidomain (MD) size. In this context, Cromwell et al. (2015) have showed the capability of subaerial basaltic volcanic glass to give accurate field intensity as they have cooled quickly and behaves as SD particles. Unfortunately, these glassy samples are not usually available, but indeed the most commonly encountered material is a lava flow which depends on its

position and cooling rate can take from days to several months to cool, and thus a wide range of domain size is expected.

All these factors may be responsible for over- or under-estimating the PI values. Xitle lava flows (Fig. 1) allowed to illustrate and discuss this problem because dozens of previous PI estimates conducted on them have commonly yielded different mean values with large dispersions . These data were mainly obtained by means of Thellier method and some others were provided by means of microwave and Shaw techniques. It should be mentioned here that previous data are of uneven quality and thus in the next section we will discuss their reliability based on today's set criteria parameters (Paterson et al., 2014; Thellier et al., 2014). The present work was designed to reinforce Xitle PI estimates and to reduce its errors through applying MSP-DSC method along one vertical (*ca*. 4.5m) and three horizontal profiles. Providing a new reliable PI value for a dated flow unit is important to (among others) enhance the global harmonic spherical models of the secular variation of the geomagnetic field over the last millennia (e.g. Nilsson et al., 2014 and Pavón-Carrasco et al., 2014) and improve our knowledge of the local field intensity behavior in central Mexico at *ca.* 370 AD.

2. Geological setting and sampling

The study profile (19.328° N; 99.189° W) is part of the flow VI of Xitle (Fig. 1) located inside the campus of UNAM (Universidad Nacional Autónoma de Mexico). Xitle lies in the central sector of the Trans-Mexican Volcanic Belt (TMVB, Fig. 1) which is an E–W trending zone of *ca.*1000 km length extending from the Pacific Ocean to the Gulf of Mexico. The TMVB is divided in western, central, and eastern sectors. The Sierra de Chichinautzin Volcanic Field (SCVF) is located in the central sector (inset Fig. 1).

The SCVF contains high concentration of monogenetic volcanoes with about 220 Quaternary

volcanic products including cinder cones and lava flows (Siebe, 2000; Rodríguez-Trejo et al., 2019) of wide compositional range. Xitle is considered as the youngest monogenetic volcano of the SCVF with a radiocarbon age of 1530-1630 uncalibrated yr BP (cal. 370±60 AD; Siebe et al., 2004; Arce et al., 2013). Xitle eruption is an example of the impact of volcanic disaster on the human population, as supposedly it had damaged the pre-Hispanic settlements around Cuicuilco pyramid (Fig. 1) which prompted them to emigrate (Siebe, 2000), as like in the historical eruptions of the Jorullo (1759–1774 AD; Guilbaud et al., 2011; Rasoazanamparany et al., 2016; Alva-Valdivia et al., 2019) and Paricutin (1943–1952 AD; Luhr and Simkin, 1993; Pioliet al., 2008) monogenetic volcanoes.

The sampled site was selected so that the bottom and top of the lava section (Fig. 3) are visible. Sampling was done using a portable gasoline powered drill, and 72 core samples, each with 5-10 cm long and 2.5 cm diameter, were collected. In this study, four profiles (Fig. 3) were taken and distributed as follow: one vertical profile (V) of *ca.* 4.5 m thickness and composed of 43 cores; and three horizontal profiles (H) of *ca.*1.25 m length for each: top horizontal (HT) of 11 cores; middle horizontal (HM) of 10 cores; and the bottom horizontal (HB) of 11 cores.

3. Previous PI studies

Nine PI studies were conducted on Xitle lava flows by means of the double heating Thellier (Nagata et al., 1965; Urrutia-Fucugauchi, 1996; Gonzales et al., 1997; Alva Valdivia, 2005; Böhnel et al., 1997; Morales et al., 2001, 2006; Mahgoub et al., 2019); microwave (Böhnel et al., 2003); and Shaw (Urrutia-Fucugauchi, 1996; Gonzales et al., 1997) methods. Sampling in five of these studies were collected randomly and its coordinates are of low precision which makes us unable to define target flow unit in some of them. On the other hand, three

studies (Böhnel et al. , 1997; 2003; Alva-Valdivia et al., 2005) were designed so as to sample vertical profiles over a specific cooling unit.

Two studies (Böhnel et al., 2003; Mahgoub et al., 2019) were carried out on pottery fragments that were reheated by Xitle eruption and thus acquired their magnetization at the same time. Böhnel et al. (2003) have performed microwave experiments on lavas and pottery fragments, with the field applied perpendicular and parallel to the their NRMs. We note also that PI data points presented in Böhnel et al. (1997) have been re-analyzed by Böhnel et al. (2003) applying a stringent set of selection criteria. At this point, it must be stated that Böhnel et al. (1997) carried out their study rather to find out how PI varies over the Xitle flow (see section 5.2) and if there is a relation between rock magnetic properties and success rate, therefore they have not used a very strict selection criteria. Morales et al. (2006) tried to figure out the cause of PI dispersion through conducting cooling rate correction. Based on their results, a significant decrease in PI-dispersion was obtained (from 7.5 to 3.5 μT), thus they have claimed that cooling-rate effect may have a prominent role in the observed dispersion. There are two points to be mentioned in this context: the first is that Morales et al. (2006) have obtained positive and negative corrections from nearby samples (of 10-20 cm distance) that should have a very similar cooling rate. Secondly, if the change in the cooling rate is the reason for the PI-dispersion, then, reasonably, Thellier results will give less scatter than microwave approach, as the duration of each microwave step is $ca.$ 10 seconds (Hill and Shaw, 1999). Böhnel et al. (2003), though using microwave technique on a nearby profile, provided PI mean results with similar dispersion as commonly obtained in Thellier. These two points most likely rule out the effect of cooling rate as a major cause of intensity variation acquired from Xitle volcano.

In order to demonstrate the PI mean and scatter in each study and to illustrate the consistency between different studies, we plot the PI data at specimen level on Figure 2. They are 214 data points [211 derived from Thellier and microwave and 3 from Shaw method] considered acceptable by the author(s) of each work. As Figure 2 illustrates, the data from each study is highly scattered and the whole data are inconsistent as well. We note that the PI-dispersion of these studies cannot be compared as the number of data is not equal: half of data were obtained by Böhnel et al. (1997) and Alva-Valdivia et al. (2005) while Urrutia-Fucugauchi (1996) and Gonzalez et al. (1997) provided only 3 PI data points using Shaw technique. Using all data, we calculate Xitle PI mean at 64.1 μT (Fig. 2) and the 95% standard deviation (σ) is 11 μT, *ca.* 18% of the mean. Since the number of data is generously available and meet the suggestion of Biggin et al. (2003) that PI mean value of any lava flow should be based on as many samples as possible (at least five). Apparently this dispersion could be related to, among others, some problems in the experimental PI methods (especially those applied long time ago). We evaluate previous 211 Thellier and microwave - derived PI data in terms of recently proposed reliability standards (e.g. Tauxe and Staudigel 2004; Chauvin et al., 2005; Paterson et al., 2014). There are some other problems that could be seriously responsible for such dispersion, including alteration of the ferromagnetic particles, cooling rate effect, and presence of local magnetic field effects. These effects will not be addressed here.

Besides the low number of provided data, the two studies that used Shaw experiment (Urrutia-Fucugauchi, 1996; Gonzalez et al.,1997) cannot be considered reliable as they did not perform alteration tests (e.g. Tsunakawa and Shaw, 1994). In Thellier experiments, samples are heated up gradually from low (e.g. 100 °C) to high temperature (commonly below curie point) and the natural remanent magnetization (NRM) is consecutively replaced

by laboratory induced thermal remanent magnetization (TRM), in a known laboratory field. This must be done with some alteration checks (Coe et al., 1978) in order to ensure that no alteration occurred during repeated heating. Laboratory procedure of microwave method is the same as Thellier but instead of heating in a conventional oven, samples are demagnetized by exposure to high-frequency microwave (Walton et al., 1993). It has been proved by Hill et al. (2002) that microwave demagnetization is equivalent to thermal counterparts implying that sample's NRM is replaced by a laboratory induced TRM, for further details we refer to the work of Hill and Shaw (2000) and Böhnel et al. (2003). Due to similarity in experimental approaches, we have set for PI data derived from Thellier and microwave the same criteria set, which are:

1) Treated sample must have been checked for thermal alteration during heating by means of the pTRM check criterions (δCK and/or δpal);

2) The stability of the sample's NRM directions during the experiments must have been evaluated by one or all next parameters: MADanc, α, or DANG;

3) Following Biggin et al. (2003) suggestion, at least 5 specimens must have been used to compute lava flow mean intensity with $\sigma \leq 10$ μT or ≤20% of the mean.

Applying these criteria set, we found that data presented in the work of Nagata et al. (1965), Urrutia-Fucugauchi (1996), Gonzalez et al. (1997), Böhnel et al. (1997), Morales et al. (2001) do not satisfy the mentioned criteria (Fig. 2). On the other hand, studies of Böhnel et al. (2003), Alva Valdivia (2005), Morales et al. (2006), and Mahgoub et al. (2019) are reliable. We calculate the Xitle mean PI from the 134 data considered as reliable data at 62.0 μT with σ of 9.3 μT (see Fig. 2). This mean value is slightly below the mean calculated from all data

and the error is also reduced, however statistically they are indistinguishable at the 95% confidence limit.

4. Methods

Rock magnetic experiments represented by the susceptibility versus temperature (*k*-T) analyses and hysteresis measurements were done on 2-3 samples from each sampled profile in order to check the magnetic variability in both horizontal and vertical directions. Alternating field (AFD) and thermal demagnetization (THD) were measured in all the samples of each profile. *k*-T curves were carried out up to ~700°C with a Bartington-MS2 susceptibility-meter coupled with the furnace XXXX (????), and the mean Curie temperature (Tc) were defined as the inflection point after peaks in *k*. We evaluate the thermal alteration that could occur during the laboratory heating by calculating a reversibility parameter: $RP\% = \frac{kh-kc}{kh} * 100$; where *k*h and *k*c represent values of *k* at heating and cooling curves at 100°C, respectively(reference ??°). Zero RP% indicates that the heated specimen does not experience alteration. Hysteresis analyses were executed with the AGFM (Alternating Gradient Force Magnetometer) for which samples weighting 5 to 40 mg were used. The hysteresis parameters (saturation magnetization (Ms); saturation remanent magnetization (Mrs); coercive force (Hc); and coercivity of remanence (Hcr)) lead to have an idea of the magnetic domain state of the magnetic carriers, Day diagram (Day et al., 1977). AFD measurements were progressively applied from 5 to 100 mT with an AGICO LDA-3 equipment. Also, THD was carried out with ASC TD-48 thermal demagnetizer model in every 50 °C from 100 to 500 °C and then from 530 to 600 °C in 30 °C step. From the demagnetization measurements, we have calculated the median destructive field (MDF) and median destructive temperature (MDT), which defined how the alternating field and

213 temperature values of the NRM loses half of its value.

214 PI experiments were estimated with the multispecimen method (Dekkers and Böhnel, 2006)
215 through which specimens are heated only once in different DC fields directed, independently,
216 parallel to the their NRM. The original protocol includes two steps: m0 and m1. Thereafter,
217 two additional steps (m2 and m3) were proposed by Fabian and Leonhardt (2010) in order to
218 correct for the domain state effect, and one more step (m4), where we repeat m1, is proposed
219 to check for any mineralogical alteration occurred during the experiment. In this study, 37
220 specimens were taken from all profiles to conduct the original (MSP-DB; referred to Dekkers
221 and Böhnel) and corrected (MSP-DSC; referred to domain state correction) protocols.
222 Heatings were carried out by use of a new infra-red-heating ultra-fast furnace developed and
223 available in the Geosciences Montpellier laboratory, called 'FUReMAG'. The heating-
224 cooling time in the FUReMAG furnace lasts 45 minutes. Based on the *k*-T curves and THD
225 results, the set-temperature will be selected so as to ensure unblocking sufficient portion of
226 NRM. Thus, we can get steeped linear fit with small confidence limit (Monster et al., 2015a),
227 and also magneto-mineralogical alteration can be avoided. To eliminate unwanted viscous
228 component in the NRM, the specimens were heated to 100°C and cooled to room temperature
229 in zero field, before the NRM measurement (m0 step). To be consistent with this pre-
230 treatment, the low temperature pTRM[100°C,Troom] was removed in the same way after
231 each pTRM acquisition (m1, m2, m3, and m4 steps) involved in the MSP-DSC protocol. The
232 magnetic remanence was measured with a cryogenic magnetometer (2G).

233 **5. Results**

234 ***5.1 Magnetic properties***

235 The *k*-T curves (Figs.4a) indicate the presence of several magnetic minerals in distinct
236 proportion. The Tc range from 540 to > 600 °C and RP% from 4 to 80%, suggesting the

presence of magnetite (Mag), Ti-poor titanomagnetite (Ti-poor TMag), and hematite with varied reversibility degrees. In all studied samples, *k* value decrease after heating, indicating that enclosed magnetic minerals have been oxidized. We found that both Tc and RP% do not have any systematic behavior vertically or horizontally, but we can mention that HT and HM profiles have moderate to good reversibility, respectively. Specimens of HB gave dissimilar results and thus no clear conclusion can be outlined.

Hysteresis analyses show that all investigated samples are located in the range of PSD field (Fig. 4b), which may suggest presence of a mixture of SD and MD particles in different percentages. HT samples are located close together in the Day plot while those of HM and HB did not show similar consistency. We deduced from these observations that HT profile has a small homogenous PSD particles while, on the other hand, the middle and bottom profiles have somewhat larger ferromagnetic particles of widespread type and/or size. Apparently, few samples are provided this explanation and thus more samples would lead to track better the domain state along vertical and horizontal profiles. However, the recent findings of Roberts et al. (2018) should be mentioned where they find out that domain state of a sample cannot be grasped simply from the Day plot as the hysteresis parameters are based on several variables (Roberts et al., 2018).

Intensity-decay curves along the three horizontal profiles results from AFD measurements (Fig. 4c) do not show any systematic behavior (as in previous experiments), and the MDF ranges from 5 to 55 mT thus indicating the presence of varying magnetic grain composition along the three sampled profiles. The THD data (Fig. 4d) showed the appearance of common Tc point of magnetite (*ca.* 560°C) with small contribution from hematite, thus in agreement with *k*-T curves. The MDTs are from 300 to 500 °C with a tendency of HB's samples (58,

59 and 64) to have lower MDT in comparison to HT and HM. This tendency could be attributed to the presence of different Ti contents (as they have low unblocking temperature spectra) or to large magnetic minerals size in the HB samples.

To sum up, magnetic experiments showed that rock from the sampled profiles, although of limited vertical and horizontal spread, have wide range of type composition and size of the enclosed magnetic minerals.

5.2 MSP-DSC results

The multispecimen data corrected for domain state (MSP-DSC) were analyzed with MSP-Tool (Monster et al., 2015) software. The set-temperature throughout the experiments is 400°C and applied DC fields range from 10 to 80 μT. The domain state proxy (α-parameter) was set to 0.5, as proposed by Fabian and Leonhardt (2010). Credibility of the MSP results were checked by three parameters: thermal-induced alteration |εalt| parameter (Fabian & Leonhardt 2010; Monster et al. 2015b); the maximum allowed angle (θ) between the isolated NRM and acquired pTRM; and the intersection parameter (Δb) (Monster et al., 2015b), which tests whether the linear fit regression line intersects the y-axis at the theoretically predicted value of −1. In order to confirm the obtained and only reliable results, we have set $|\varepsilon alt| \leq 5\%$, θ must be less than 10°, and a threshold value of Δb is ± 0.1. In the MSP-Tool software, the bootstrap statistics were applied to calculate the mean and 95% confidence intervals.

Technically, successful MSP experiments were obtained from profiles V and HT, while both HM and HB failed to give reliable estimates as their εalt parameter exceeded the defined limit. In V, three specimens out of nine were rejected (Fig. 5a) as they have altered during the MSP run. The remaining six met the criteria limit defined above and thus a domain state corrected PI mean of $62.9 \pm 2.6\ \mu T$ was obtained for the vertical profile. The HT gave

283 successful MSP experiment in eight out of ten specimens (Fig 5b), with PI value of *58.6 μT*,
284 after DSC procedure. We note here that 95% confidence interval in HT (+6.5/-6.3 μT) is
285 almost double the value of the confidence interval in V. Obviously, this high scatter is
286 reasoned by the noticeable nonlinearity behavior, in the last field steps (Fig. 5b), between the
287 TRM and applied magnetic field. This non-ideal behavior can be attributed to presence of
288 large ferromagnetic particles, which can reduce the efficiency of linearity law (Selkin et al.,
289 2007). Regarding to HM, only one specimen out of nine passed the alteration limit (Fig. 5c),
290 indicating that most of the middle-zone specimens are susceptible to alteration. In addition,
291 the last data points are not aligned linearly which probably point to the dominance of MD
292 particles. Therefore, no reliable results were obtained from this profile.
293 We have neglected the criteria limits to obtain reliable results without regard to data quality,
294 just to see the impact of the sample position in vertical profile on the PI results. A MSP-DSC
295 value of *67.2 μT* was obtained, this is demonstrated in the supplementary Figure S1. Three
296 accepted data out of nine (33% success rate) was found along HB profile (Fig. 5d) and thus
297 no meaningful estimate could be obtained. As in HM, if we neglect the criteria set parameters
298 (Fig. S2), a value of *60.8 μT* is calculated for HB profile.
299 From the above results, it is obvious that only the vertical and upper horizontal profiles gave
300 reliable results that meet the proposed criteria limits. Therefore, combining all accepted
301 specimens from V and HT enables us to assign Xitle-mean PI (Fig. 6a) at *60.5 (+4.0/-4.1)*
302 *μT*. Including all the 18 specimens of HM and HB (Fig. 6b) gives, unexpectedly, a mean
303 value of *63.8 (+5.2/-5.8)* μT, which considering the uncertainty limits, is indistinguishable
304 from the mean value calculated from only reliable results. This consistency may denote that
305 the current conditions set for accepting the MSP results (εalt and Δb) are ineffective. Such

306 explanation, however, cannot be confirmed in this study, as the actual intensity value during
307 Xitle eruption time (370 AD) is unknown. But, we can deduce that obtaining reliable MSP
308 results for a certain lava unit could be achieved by taking many specimens as possible from
309 different parts within the lava flow. However, these approaches will costs effort and time.

310 **6. Discussion**

311 Three horizontal profiles were sampled from Xitle in three levels from bottom to top in order
312 to discuss horizontal variations of paleointensity. Horizontal characteristics along these
313 profiles were investigated as well through sampling one vertical profile of *ca.* 4.5 m
314 thickness. Rock magnetic experiments were completed to infer the type and size of the
315 ferromagnetic minerals and their thermal stability. It must be mentioned that the number of
316 present samples that have undergone magnetic experiments and MSP run are few and uneven,
317 and thus the relationship between magnetic properties and paleointensity behavior along
318 lava's profile may not be clear. However is not the main focus of this study, as we here try
319 to enhance the PI estimates of Xitle by evaluating previous data and conducting a new MSP
320 experiment. Completing this, we can provide an average value with low confidence limit,
321 through combining present PI results with reliable results obtained from previous studies.
322 Despite the limited number of data, we can give a general overview of the impact of lava
323 position and its physical and magnetic properties on the MSP results. Currently, few studies
324 have addressed the relation between rock magnetic properties and lava flow thickness. Some
325 studies (Coe et al., NATURE, 1995; Rolph, 1997; Hill and Shaw, 2000; Vérard et al., 2012)
326 have discussed this relation on thin lava flows, thickness < 2 m, some others extended these
327 studies to thicker lavas of ~6m long (Böhnel et al., 1997; de Groot et al., 2014), and up to
328 several tens of meters (e.g. Wilson et al., 1968; Audunssen et al., 1992). Findings from these

studies indicate an effect of the sampling location on the magnetic properties. Lava thickness reflects different cooling history, the top and bottom parts cooled faster than the central part of the flow. These variations in cooling time govern the size of the ferromagnetic crystals and their oxidations states. The top part of the lava flows may produce smaller ferromagnetic sensus lato particles with lower oxidation state in comparison to those formed in the middle of the flow (see for example Böhnel et al., 1997; de Groot et al., 2014).

Böhnel et al. (1997) showed detailed results of Xitle's rock magnetic properties (i.e. Tc, magnetic susceptibility, hysteresis parameters, and coercivities) and PIs along a vertical profile of 6 m thickness. Results indicate that, unlike magnetic properties, the PIs seem to have a systematic behavior with tendency of middle flow samples to give larger PI variations in comparison to the top and bottom samples. Despite the detailed study, they did not find meaningful relation between PI variations and physical and magnetic properties. Our sampled profile spaced only (0.96 km) from Böhnel et al. (1997) profile, implying that they shared almost the same cooling history. The rock-magnetic experiments done in this study showed that Ti-poor TMt and/or Mt is the dominant ferromagnetic mineral(s) and few hematite is present, showed from *k*-T curves (Fig. 4a). These minerals are located broadly on the PSD size with wide range of MDF (from *ca.* 5 to 56 mT). From top to bottom (V), and along each horizontal profile (HT, HM, HB), we do not find any systematic changes on the magnetic properties although of the, above mentioned, differences in cooling times. Although the magnetic parameters obtained in this study varied (e.g. RP%, MDF and MDT) horizontally, we consider that they do not reflect true magnetic properties changes, as the cooling time and content of the cooled lava on such a small scale (1.5 m) are seemingly constant, at least in comparison to vertical direction. This discrepancy in magnetic data could

be attributed to the limited number of rock magnetic experiments carried out. In conclusion, there is not a direct connection found between lava thickness and its 1.5 m lateral extent with the magnetic properties.

Now, we discuss the influence of cooling time on the MSP results. Our contributed results show that the topmost horizontal profile and the vertical profile have yielded successful MSP-DSC PI determinations from the 14 selected samples out of 19 available (74% success rate). On the hand, samples from central and bottom parts of the flow do not give satisfactory MSP results, as they have exceeded the limits of criteria set designed following Monster et al. (2015). Apparently, getting differential MSP results and success rate from over a flow section of 4.5 m thickness can be directly related to the cooling time of this flow. It means that top part of the Xitle flow is appropriate for conducting MSP experiments as it has cooled faster than underlying horizontal sections. Moreover, conducting the experiment vertically does give almost the same results given from HT profile (Fig. 5a and b), which could indicate that the effect of cooling time on MSP results may be insignificant or even disappeared if samples are taken vertically. This explanation is based on a few number of samples and more studies are needed to emphasize it. From these notes, we recommend sampling a lava flow horizontally from its top part when the lava flow is notovered by a younger flow, and vertically in order to give a reliable MSP estimates.

7. Conclusions

The rock magnetic properties indicate that the main magnetic minerals are Ti-poor titanomagnetite with small contribution from hematite of PSD carriers accomplish the quality

criterion to be able for paleointensity experiments.

Successful MSP-DSC experiments were obtained from profiles V and HT, while both HM and HB failed to give reliable estimates. Results obtained in this study from 14 accepted specimens of HT and V profiles give an average mean for Xitle at *60.5 (+4.0/-4.1) μT*. This value constrains greatly the dispersion and we consider it should substitute the value for the Xitle from the database used by models in order to do more precise the secular variation curve used for the dating of geologic and archeomagnetic materials of this period.

This mean value is consistent with the mean (*62.0 ± 9.3 μT*) calculated from 134 filtered Thellier & microwave old PI data. The whole PI mean value for Xitle, using a combined formula (Higgins and Green, 2011) gives 61.9 ± 9 μT. This mean value is calculated from high quality data provided from three different PI methods, therefore most likely represents the intensity value for Central Mexico at *ca.* 370 AD.

Acknowledgments

We appreciate the financial support to L. M. Alva-Valdivia from PAPIIT-DGAPA-UNAM IN113117 and ANR-CONACyT (France-Mexico) 273564, research projects. AN Mahgoub acknowledged the financial support of the Universidad Nacional Autónoma de México-postdoctoral fellowship. M. A. Bravo-Ayala was partly financially supported by a scholarship from CONACyT and a Research Grant from Dr. P. Camps and Dr. T. Poidrás whom allowed the use of the Paleomagnetic laboratory of Geoscience University of Montpellier, France. Thanks to J. A. González Rangel for the support on the Mexican Paleomagnetic laboratory experiments.

References

Aitken, M., Allsop, A., Bussell, G., Winter, M., 1988. Determination of the intensity of the Earth's magnetic field during archaeological times: Reliability of the Thellier technique. Rev. Geophys. 26 (1), 3–12.

Alva-Valdivia, L., 2005, Comprehensive paleomagnetic study of a succession of Holocene olivine-basalt flow: Xitle Volcano (Mexico) revisited, Earth Planets Space, Vol. 57, pp. 869-853.

Audunssen, H., S. Levi, and F. Hodges (1992), Magnetic property zonation in a thick lava flow, J. Geophys. Res., 97(B4), 4349–4360.

Biggin, A.J., Steinberger, B., Aubert, J., Suttie, N., Holme, R., Torsvik, T.H., van der Meer, D.G., van Hinsbergen, D.J.J. (2012) Possible links between long-term geomagnetic 644 variations and whole-mantle convection processes. Nat Geosci 5:526–533

Biggin, A.J., Böhnel, H.N. & Zuniga, F.R., 2003. How many paleointensity determinations are required from a single lava flow to constitute a reliable average? Geophys. Res. Lett., 30(11).

Böhnel, H., Morales, J., Caballero, C., Alva, L., McIntosh, G., González, S. y Sherwood, J., 1997, Variation of rock magnetic parameters and paleointensities over a single holocene lava flow, J. Geomag. Geoelectr., 49, 523 - 542.

Böhnel, H., E. Herrero-Bervera, and M. J. Dekkers (2011), Paleointensities of the Hawaii 1955 and 1960 Lava Flows: Further Validation of the Multi-specimen Method, pp. 195–211, Springer, Dordrecht, Netherlands.

Böhnel, H., A. J. Biggin, D. Walton, J. Shaw, and J. A. Share (2003), Microwave palaeointensities from a recent Mexican lava flow, baked sediments and reheated pottery, Earth Planet. Sci. Lett., 214, 221–236.

Coe, R.S., 1967. Paleo-intensities of the Earth's magnetic field determined from Tertiary and Quaternary rocks. J. Geophys. Res. 72 (12), 3247–3262.

Coe RS, Grommé S, Mankinen EA (1978) Geomagnetic paleointensities from radiocarbon dated lava flows on Hawaii and the question of the Pacific nondipole low. J Geophys Res Solid Earth 83(B4):1740–1756

Cromwell, G., Tauxe, L., Staudigel, H., Ron, H., 2015. PI estimates from historic and modern Hawaiian lava flows using glassy basalt as a primary source material. Phys. Earth Planet. Inter.241, 44–56.

de Groot, L. V., T. A. T. Mullender, and M. J. Dekkers (2013), An evaluation of the influence of the experimental cooling rate along with other thermomagnetic effects to explain anomalously low palaeointensities obtained for historic lavas of Mt Etna (Italy), Geophys. J. Int., 193(3), 1198–1215, doi:10.1093/gji/ggt065.

de Groot, L.V., Dekkers, M.J., Visscher, M., ter Maat, G.W., 2014. Magnetic properties and paleointensities as function of depth in a Hawaiian lava flow. Geochem. Geophys. Geosyst.15. http://dx.doi.org/10.1002/2013GC005094.

Day, R., Fuller, M., Schmidt, V.A., 1977. Hysteresis properties of titanomagnetites: grain size and compositional dependence. Phys. Earth Planet. Inter. 13, 260–267.

Dekkers, M.J., Böhnel, H.N., 2006. Reliable absolute palaeointensities independent of magnetic domain state. Earth Planet. Sci. Lett. 284, 508-517.

Dunlop, D.J., 2002. Theory and application of the Day plot (Mrs/Ms versus Hcr/Hc) 1. Theoretical curves and tests using titanomagnetite data. J. Geophys. Res 107(B3) 2056. doi:10.1029/2001JB000486.

Fabian, K., Leonhardt, R., 2010. Multiple-specimen absolute PI determination: An optimal protocol including pTRM normalization, domain-state correction, and alteration test. Earth Planet. Sci. Lett. 297, 84–94.

Gonzalez S, Sherwood GJ, Boehnel H, Schnepp E (1997), Paleosecular variation in central Mexico over the last 30,000 years: The record from lavas. Geophys J Int 130: 201– 219.

González, S., Pastrana, A., Siebe, C., Duller, G., 2000. Timing of the prehistoric eruption of Xitle volcano and the abandonment of Cuicuilco pyramid, southern Basin of Mexico. Geol. Soc. London Sp. Pub. 171, 205-224. https://doi.org/10.1144/GSL.SP.2000.171.01.17.

Grappone, J.M., Biggin, A.J., Hill. M.J., 2019: Solving the mystery of the 1960 Hawaiian lava flow: implications for estimating Earth's magnetic field. Geophys. J. Int., 218, 1796–1806.

462 Guilbaud, M.N., Siebe, C., Layer, P., Salinas, S., 2012. Reconstruction of the volcanic history
463 of the Tacámbaro-Puruarán area (Michoacán, México) reveals high frequency of
464 Holocene monogenetic eruptions. Bull. Volcanol. 74, 1187–1211.
465
466 Heizer, R.F., Bennyhoff, J.A., 1958. Archeological investigations of Cuicuilco, Valley of
467 Mexico, 1957. Science 127, 232±233.
468 Higgins J and Green S. Cochrane Handbook for Systematic Reviews of Interventions
469 Version 5.1.0. The Cochrane Collaboration, 2011, www.handbook.cochrane.org.
470 Hill, M. J., and J. Shaw (1999), Palaeointensity results for historic lavas from Mt Etna using
471 microwave demagnetization/remagnetization in a modified Thellier-type
472 experiment, Geophys. J. Int., 139(2), 583–590
473 Hill, M. J., and J. Shaw (2000), Magnetic field intensity study of the 1960 Kilauea lava flow,
474 Hawaii, using the microwave PI technique, Geophys. J. Int., 142, 487–504.
475 Luhr, J.F., Simkin, T., 1993. Paricutin: The Volcano Born in a Mexican Cornfield.
476 Geoscience Press (427 p).
477 Mahgoub, A.N., Juárez-Arriaga, E., Böhnel, H., Manzanilla, L.R., Cyphers, A., 2019.
478 Refined 3600 years palaeointensity curve for Mexico. Phys. Earth Planet. Inter.
479 Accepted.
480 Morales, J., Alva-Valdivia, L., Goguitchaichvili, A. y Urrutia-Fucugauchi, J., 2006, Cooling
481 rate corrected paleointensities from the Xitle lava flow: Evaluation of within-site
482 scatter for single spot-reading cooling units, Earth Planets Space, Vol. 58, pp. 1341-
483 1347.
484 Morales, J., Goguitchaichvili, A. y Urrutia-Fucugauchi, J., 2001, A rock-magnetic and PI
485 study of some Mexican volcanic lava flows during the Latest Pleistocene to the
486 Holocene, Earth Planets Space, Vol. 53, pp. 893–902.
487 Monster, M.W.L., de Groot, L.V., Biggin, A.J., Dekkers, M.J., 2015a. The performance of
488 various PI techniques as a function of rock magnetic behaviour – a case study for
489 La Palma. Phys. Earth Planet. Inter. 242, 36–49. http://dx.doi.org/10.1016/
490 j.pepi.2015.03.004

Monster, M.W.L., de Groot, L.V., Dekkers, M.J., 2015b. MSP-tool: a VBA-based software tool for the analysis of multispecimen PI data. Front. Earth Sci. 3, 86. http://dx.doi.org/10.3389/feart.2015.00086.

Nagata, T., Kobayashi, K., Schwarz, E.J., 1965. Archaeomagnetic intensity studies of South and Central America. J. Geomagnetism Geoelectricity, 17, 399-405, https://doi.org/10.5636/jgg.17.399

Nilsson A, Holme R, Korte M, Suttie N, Hill M (2014) Reconstructing Holocene geomagnetic field variation: New methods, models and implications. Geophys J Int 198(1):229–248

Paterson GA, Tauxe L, Biggin AJ, Shaar R, Jonestrask LC (2014) On improving the 843 selection of Thellier-type paleointensity data. Geochem Geophys Geosyst 15(4): 1180–844 1192

Paterson, G. A., L. Tauxe, A. J. Biggin, R.Shaar, and L. C. Jonestrask (2014), On improving the selection of Thellier-type paleointensity data, Geochem.Geophys. Geosyst., 15, 1180–1192,doi:10.1002/2013GC005135.

Pavón-Carrasco, F.J., Osete, M.L., Torta, J.M., De Santis, A., 2014. A geomagnetic field model for the Holocene based on archaeomagnetic and lava flow data. Earth Planet. Sci. Lett. 388, 98–109.

Pioli, L., Erlund, E., Johnson, E., Cashman, K.V., Wallace, P., Rosi, M., Delgado, H., 2008. Explosive dynamics of violent Strombolian eruptions: the eruption of Paricutin volcano 1943–1952 (Mexico). Earth Planet. Sci. Lett. 271 (1–4), 359–368.

Rasoazanamparany, C., Widom, E., Siebe, C., Guilbaud, M.-N., Spicuzza, M.J., Valley, J.W., Valdez, G., Salinas, S., 2016. Temporal and compositional evolution of Jorullo volcano, Mexico: implications for magmatic processes associated with a monogenetic eruption. Chem. Geol. 434, 62–80.

Rolph, T.C., 1997. An investigation of the magnetic variation within two recent lava flows, Geophys. J. Int., 130, 125–136.

Roberts, A.P., Tauxe, L., Heslop, D., Zhao, X., Jiang, Z., 2018. A critical appraisal of the Day diagram. J. Geophys. Res. 123, 2618–2644. https://doi.org/10.1002/2017JB015247.

Selkin, P. A., J. S. Gee, and L. Tauxe (2007), Nonlinear thermoremanence acquisition and implications for PI data, Earth Planet. Sci. Lett., 256, 81–89, doi:10.1016/j.epsl.2007.01.017.

Siebe, C., 2000. Age and archaeological implications of Xitle volcano, southwestern Basin of Mexico-City. J. Volcanol. Geotherm. Res. 104, 45-64. https://doi.org/10.1016/S0377-0273(00)00199-2.

Shaw, J., 1974, A new method of determining the magnitude of the paleomagnetic field application to 5 historic lavas and five archeological samples. Geophysical Journal of the Royal Astronomical Society 39: 133-141. doi: 10.1111/j.1365-246X.1974.tb05443.x.

Stacey, F.D. & Banerjee, S.K., 1974. The Physical Principles of Rock Magnetism, Elsevier, Amsterdam.

Tauxe, L., T. Pick, and Y. Kok (1995), Relative PI in sediments: A pseudo-Thellier approach, Geophys. Res. Lett., 22(21), 2885–2888.

Thellier, E. & Thellier, O., 1959. Sur l'intensité du champ magnétique terrestre dans le passé historique et géologique, Ann Géophys., 15, 285–376.

Tauxe, L., Staudigel, H., 2004. Strength of the geomagnetic field in the Cretaceous Normal Superchron: new data from submarine basaltic glass of the Troodos Ophiolite. Geochem. Geophys. Geosyst. 5 (Q02H06).

Tsunakawa, H., Shaw, J., 1994. The Shaw method of PI determinations and its application to recent volcanic rocks. Geophys. J. Int. 118, 781–787.

Urrutia Fucugauchi, J., 1996. Palaeomagnetic study of the Xitle- Pedregal de San Angel lava flow, southern Basin of Mexico. Physics of the Earth and Planetary Interiors 97, 177-196.

Verard, C., R. Leonhardt, and M. Winklhofer (2012), Variations of magnetic properties in thin lava flow profiles: Implications for the recording of the Laschamp Excursion, Phys. Earth Planet. Inter., 200–201, 10–27, doi:10.1016/j.pepi.2012.03.012.

Walton, D., Share, J.A., Rolph, T.C. & Shaw, J., 1993. Microwave magnetisation, Geophys. Res. Lett., 20, 109–111.

Wilson, R. L., S. E. Haggerty, and N. D. Watkins (1968), Variation of palaeomagnetic stability and other parameters in a vertical traverse of a single Icelandic lava, Geophys. J. R. Astron. Soc., 16, 79–96.

Yamamoto,Y., Tsunakawa,H.&Shibuya, H., 2003. Palaeointensity study of the Hawaiian 1960 lava: implications for possible causes of erroneously high intensities, Geophys. J. Int., 153(1), 263–276.

List of Figures

Figure 1. Distribution of Xitle lava flows I to VI, with the location of the sampling site and the Cuicuilco archeological site. Modified after Delgado et al. (1998).

Figure 2. Evaluation of previous PI data published for Xitle. The closed and open circles represent reliable and unreliable data based on a set of selection criteria designed in this study (see section 2). The dotted line and shaded area is the Xitle mean paleointensity value and 95% standard deviation, calculated from only reliable data. the x-axis represent different studies that were done on Xitle.

for abbreviations: *Nag-65* is Nagata et al. (1965); *UFT-96* is Urrutia-Fucugauchi (1996), from thellier experiment; *UFS-96* is Urrutia-Fucugauchi (1996) from Shaw experiment; *BH-97* is Böhnel et al. (1997); *GZT-97* is Gonzales et al. (1997) from thellier; *GZS-97* is Gonzales et al. (1997) from Shaw; *M-01* is Morales et al. (2001); *BHT-03* is Böhnel et al. (2003) from thellier after re-analyzing data of Böhnel et al. (1997*); BHMl-03* is Böhnel et al. (2003) from microwave done on lavas; *BHMp-03* is Böhnel et al. (2003) from microwave done on potteries; *LA-05* is Alva-Valdivia (2005); *M-06* is Morales et al. (2006); and *MG-19* is Mahgoub et al. (2019, accepted for publication).

Figure 3. Sampling profile. Lava flow with scale (1m). Three zones are observed with the naked eye: the massive central zone and the upper zone that present abundant vesicles and lower with much less and tiny vesicles. The core numbers are shown in order to be compared with upcoming rock magnetic properties and paleointensities.

Figure 4. Rock magnetic results done in this study: (a) susceptibility vs. temperature curves; (b) Day plot (Day et al., 1977) with thresholds for single domain (SD), pseudo single domain (PSD), and multidomain (MD) shown as straight grey lines. Dashed curved lines represent the SD-MD theoretical mixing curves, after Dunlop (2002); (c) intensity decay curves obtained after alternating field demagnetization; (d) intensity decay curves after thermal demagnetization. Numbers in each panel diagram represent core sample, see Figure 3. AHMED, LAS CURVAS EN 4A CASI NO SE VEN. Y EN 4C Y 4D EL EJE Y DEBE SER NORMALIZED MAGNETIZATION.

Figure 5. Multispecimen results obtained from four sampled profiles, after domain state correction (DSC). In each DSC protocol, the average alteration parameter (εalt) and the intersection criterion (Δb) are demonstrated to judge the credibility of the given results. Note that data were analyzed with MSP-Tool software (Monster et al., 2015b) where bootstrap statistics were applied to calculate the mean (solid black line) and 95% confidence interval (dashed black lines lines). Black and orange circles represent those accepted and unaccepted data, respectively, based on the criteria limit defined in the present study. (a and b) represent accepted experiments done on profiles V and HT, as their specimens meet the designed criteria limit, and (c and d) represent unaccepted experiments from profiles HM and HB and thus no PI mean could be calculated from these two profiles.

Figure 6. (a) Xitle PI mean value calculated from only reliable experiments done on V and HT profiles. (b) represents unreliable experiments (from profiles HM and HB), and the bootstrap mean (solid black line) and 95% confidence interval (dashed black lines lines) are shown to compare the Pi results obtained from reliable (a) and unreliable (b) data.

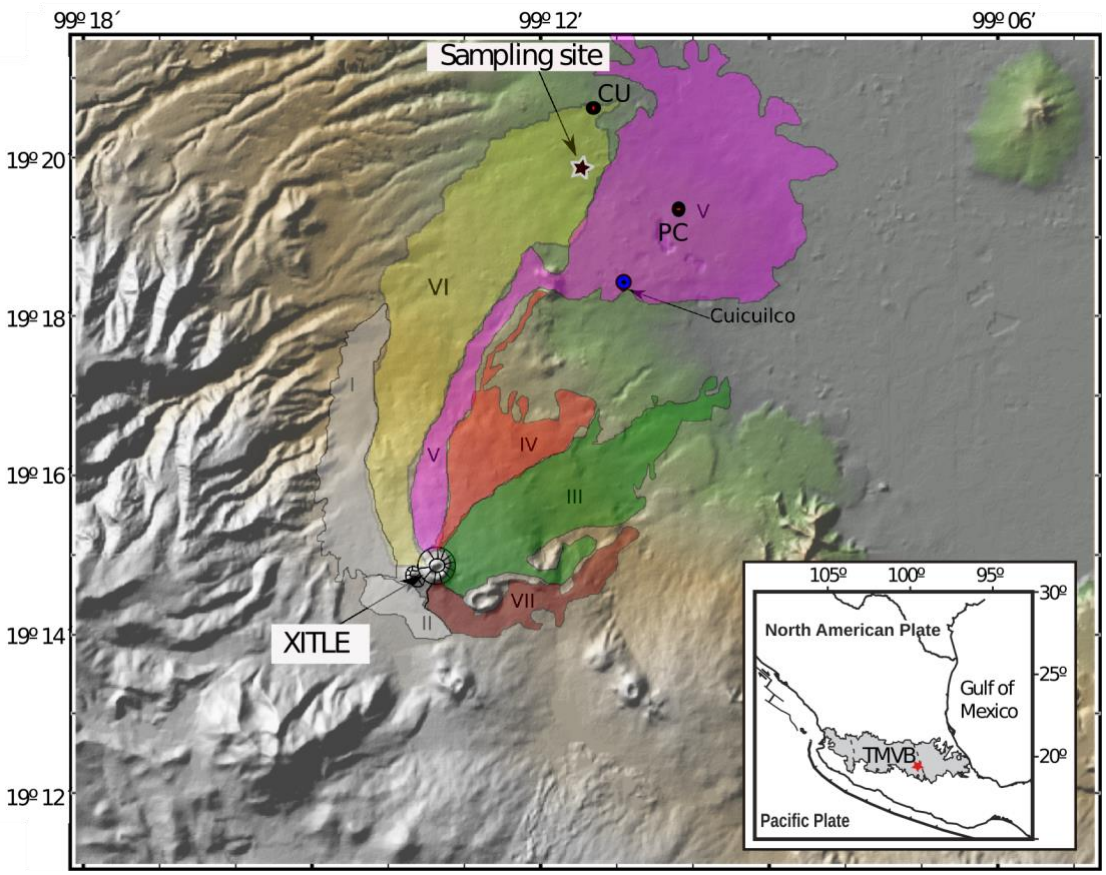

Figure 1. Distribution of Xitle lava flows I to VI, with location of the sampling site and Cuicuilco archeological site. Modified after Delgado et al. (1998). WE ARE STILL WORKING ON THIS FIGURE!

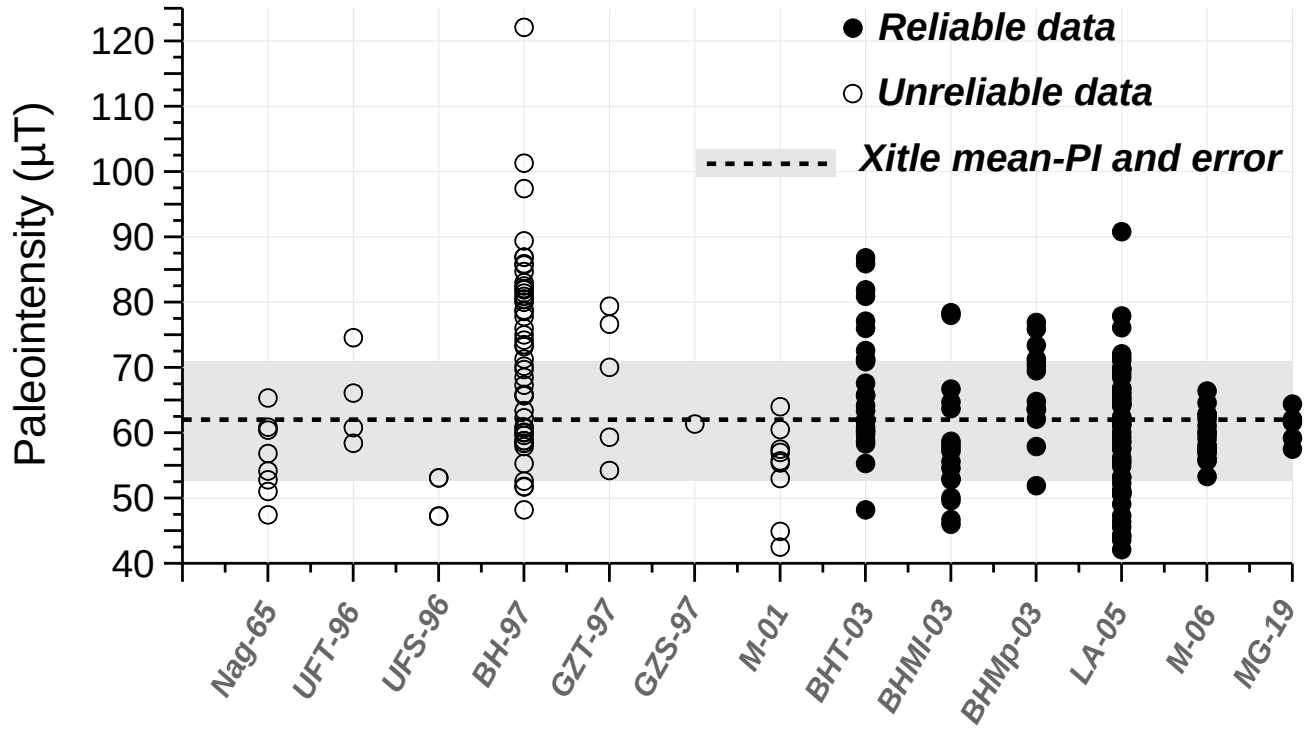

Figure 2. Evaluation of previous PI data published for Xitle. The closed and open circles represent reliable and unreliable data based on a set of selection criteria designed in this study (see section 2). The dotted line and shaded area is the Xitle mean paleointensity value and 95% standard deviation, calculated from only reliable data. the x-axis represent different studies that were done on Xitle.

for abbreviations: *Nag-65* is Nagata et al. (1965); *UFT-96* is Urrutia-Fucugauchi (1996), from thellier experiment; *UFS-96* is Urrutia-Fucugauchi (1996) from Shaw experiment; *BH-97* is Böhnel et al. (1997); *GZT-97* is Gonzales et al. (1997) from thellier; *GZS-97* is Gonzales et al. (1997) from Shaw; *M-01* is Morales et al. (2001); *BHT-03* is Böhnel et al. (2003) from thellier after re-analyzing data of Böhnel et al. (1997*); BHMl-03* is Böhnel et al. (2003) from microwave done on lavas; *BHMp-03* is Böhnel et al. (2003) from microwave done on potteries; *LA-05* is Alva-Valdivia (2005); *M-06* is Morales et al. (2006); and *MG-19* is Mahgoub et al. (2019, accepted for publication).

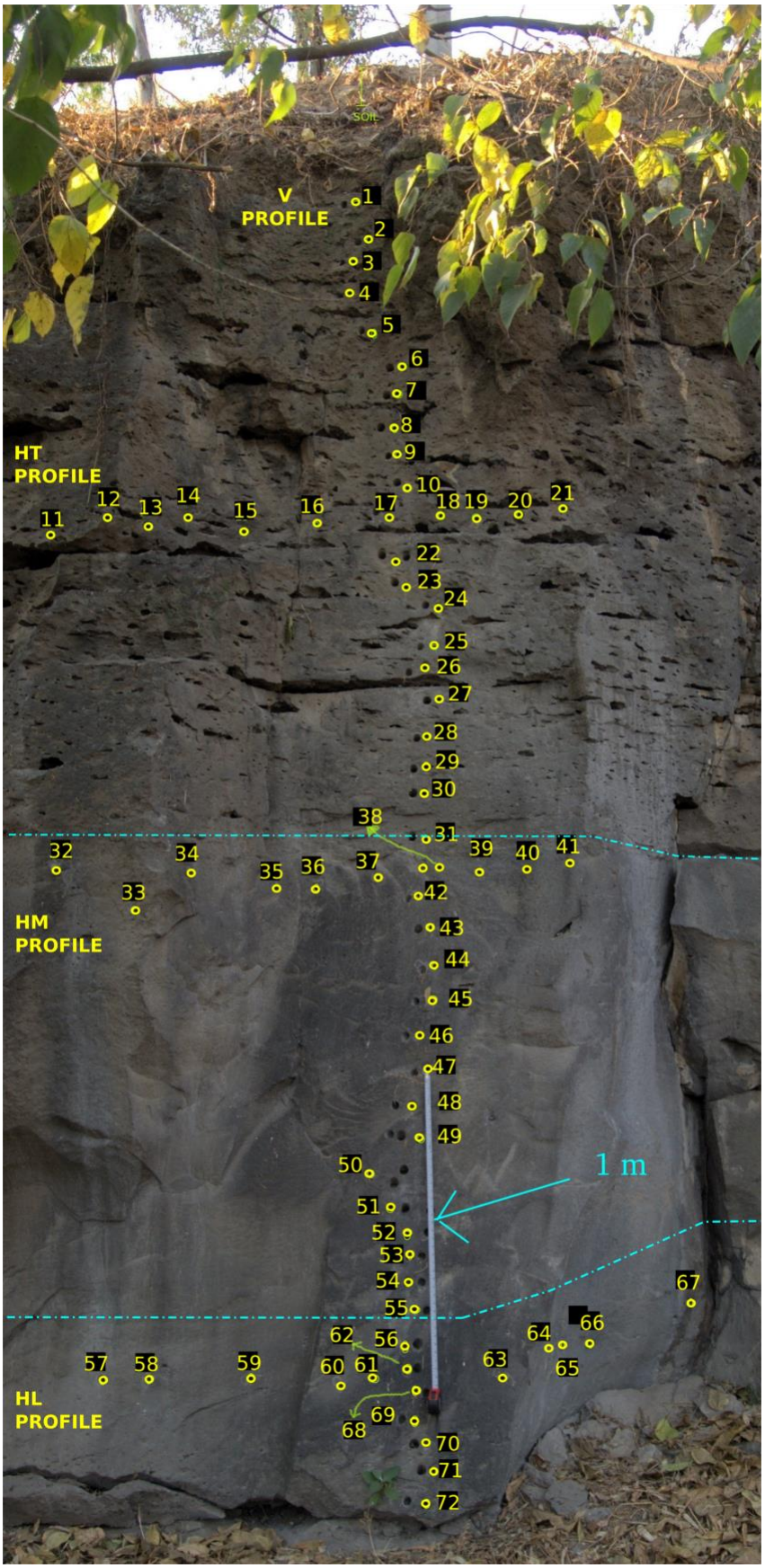
V
PROFILE
HT
PROFILE
HM
PROFILE
HL
PROFILE
1 m
1
2
3
4
5
6
7
8
9
10
11
12
13
14
15
16
17
18
19
20
21
22
23
24
25
26
27
28
29
30
31
32
33
34
35
36
37
38
39
40
41
42
43
44
45
46
47
48
49
50
51
52
53
54
55
56
57
58
59
60
61
62
63
64
65
66
67
68
69
70
71
72

Figure 3. Sampling profile. Lava flow with scale (1m). Three zones are observed with the naked eye: the massive central zone and the upper and lower zones that present vesicles. The core numbers are shown in order to be compared with upcoming rock magnetic properties and paleointensities.

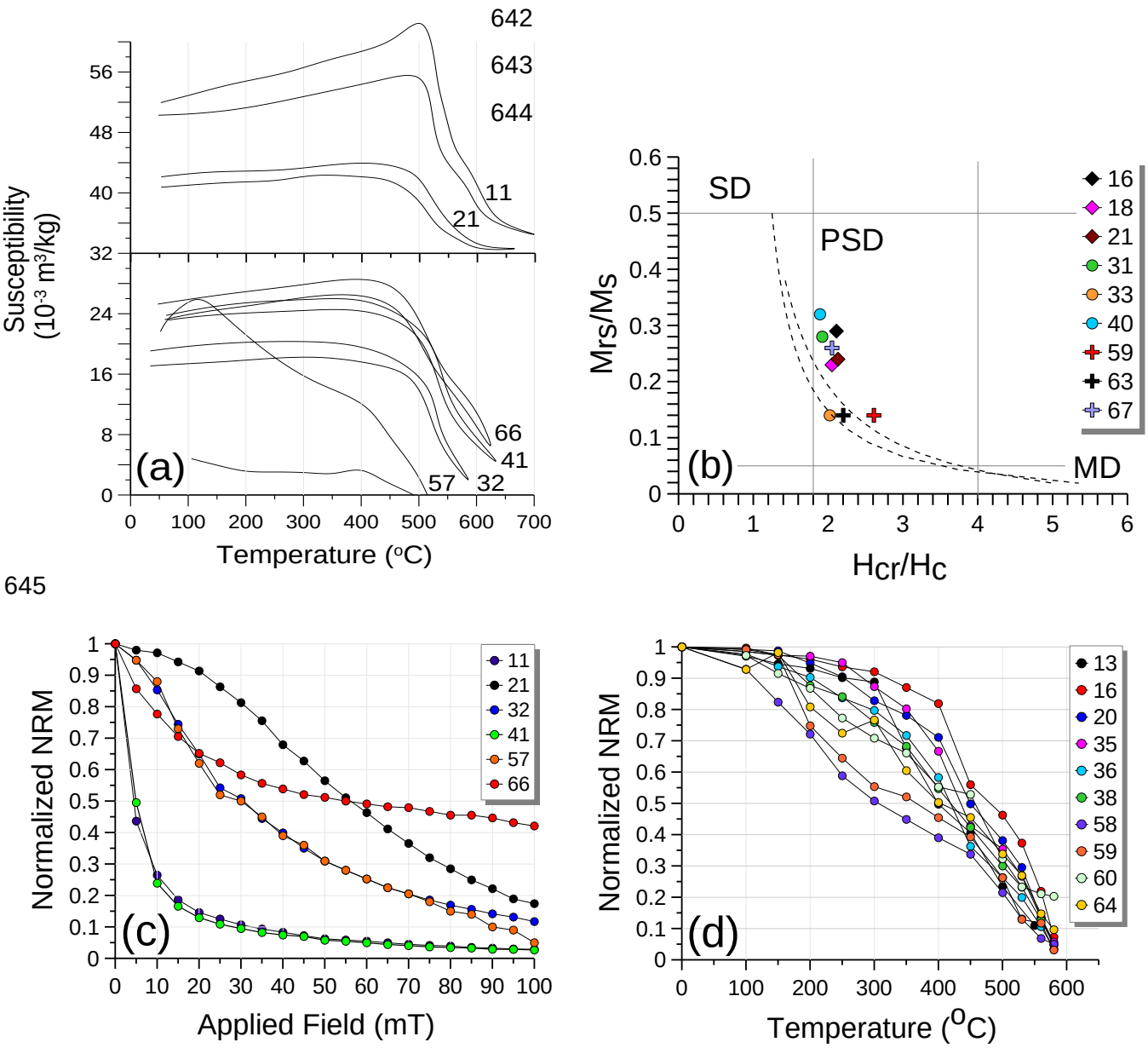

Figure 4. Rock magnetic results done in this study: (a) susceptibility vs. temperature curves; (b) Day plot (Day et al., 1977) with thresholds for single domain (SD), pseudo single domain (PSD), and multidomain (MD) shown as straight grey lines. Dashed curved lines represent the SD-MD theoretical mixing curves, after Dunlop (2002); (c) intensity decay curves obtained after alternating field demagnetization; (d) intensity decay curves after thermal demagnetization. Numbers in each panel diagram represent core sample, see Figure 3.

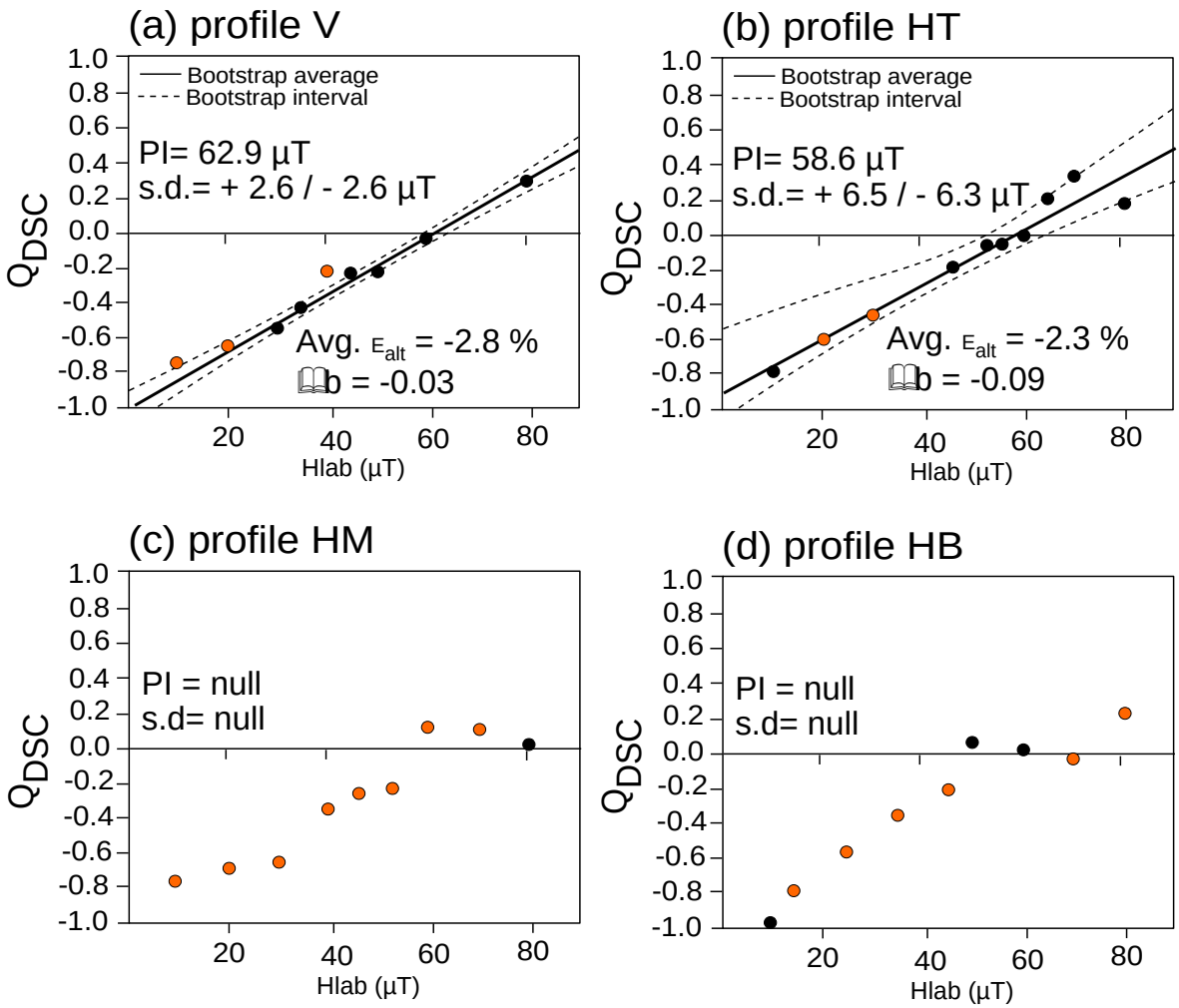

655

656

657

658

659

660 **Figure 5**. Multispecimen results obtained from four sampled profiles, after domain state
661 correction (DSC). In each DSC protocol, the average alteration parameter (εalt) and the
662 intersection criterion (Δb) are demonstrated to judge the credibility of the given results. Note
663 that data were analyzed with MSP-Tool software (Monster et al., 2015b) where bootstrap
664 statistics were applied to calculate the mean (solid black line) and 95% confidence interval
665 (dashed black lines lines). Black and orange circles represent those accepted and unaccepted
666 data, respectively, based on the criteria limit defined in the present study. (a and b) represent
667 accepted experiments done on profiles V and HT, as their specimens meet the designed

668 criteria limit, and (c and d) represent unaccepted experiments from profiles HM and HB and
669 thus no PI mean could be calculated from these two profiles.
670

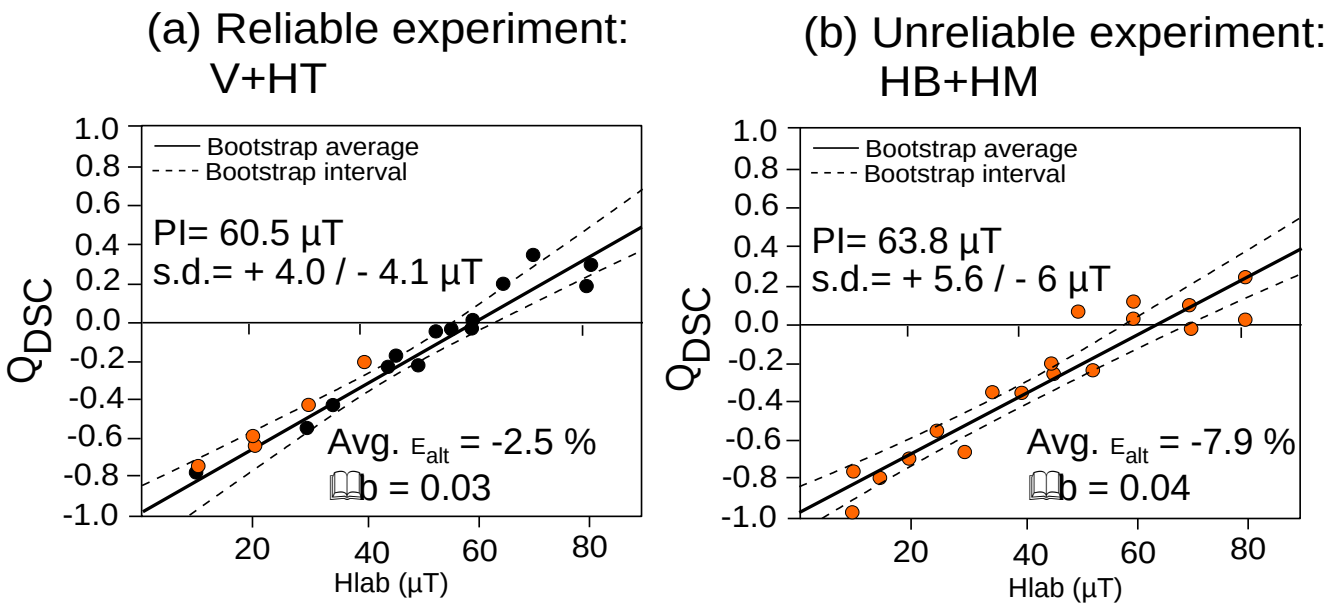

Figure 6. (a) Xitle PI mean value calculated from only reliable experiments done on V and HT profiles. (b) represents unreliable experiments (from profiles HM and HB), and the bootstrap mean (solid black line) and 95% confidence interval (dashed black lines lines) are shown to compare the Pi results obtained from reliable (a) and unreliable (b) data

Supplementary Materials

The supplementary materials consist of two figures.

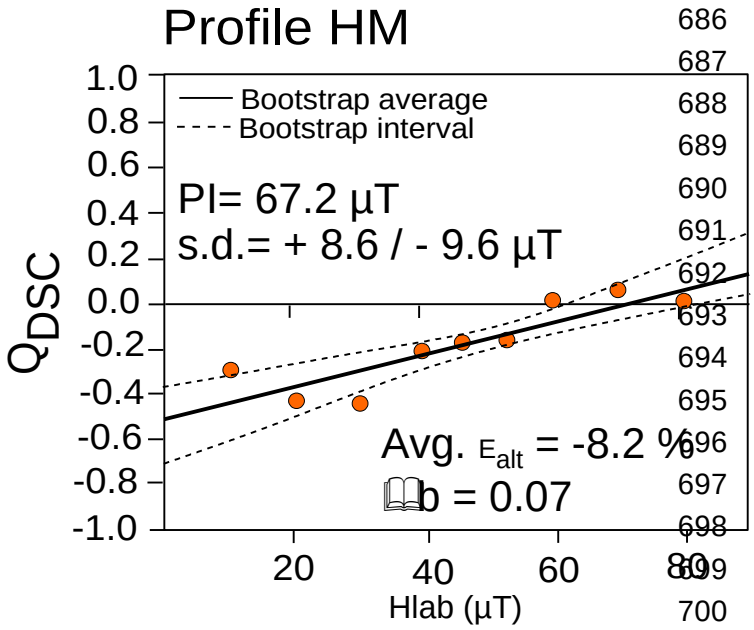

Figure S1. Multispecimen results obtained from central profile (HM), after domain state correction (DSC). The data were analyzed with MSP-Tool software (Monster et al., 2015b) where bootstrap statistics were applied to calculate the mean (solid black line) and 95% confidence interval (dashed black lines lines). We note that in this profile we do not apply the selection criteria defined in the present study, as we just need to compare the unreliable data with reliable data.

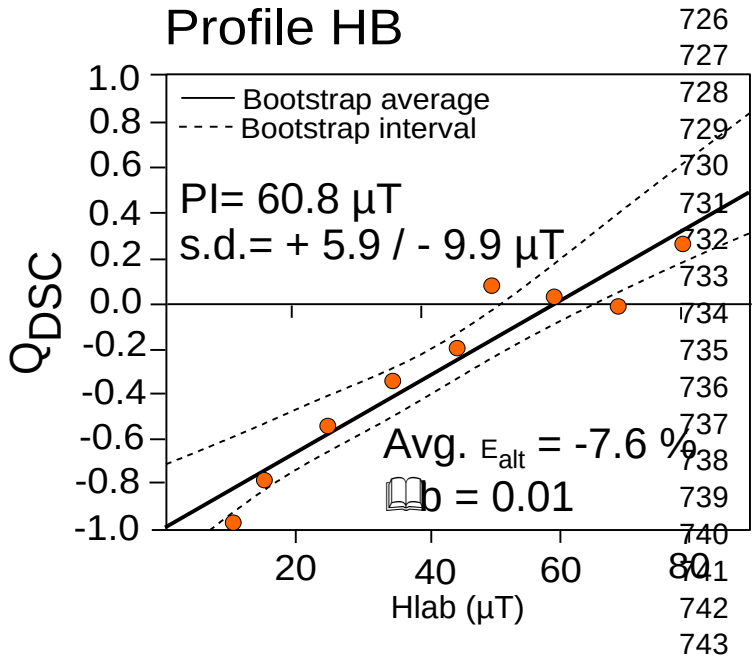

Figure S2. Multispecimen results obtained from bottom profile (HB). For details see Fig. S2 caption.